When Adjacent Lane Dependencies Dominate the Uncongested Regime of the Fundamental Relationship

Balaji Ponnu

Graduate Research Assistant
The Ohio State University
Department of Civil, Environmental, and Geodetic Engineering

Benjamin Coifman, PhD

Associate Professor
The Ohio State University
Joint appointment with the Department of Civil, Environmental, and Geodetic Engineering, and the Department of Electrical and Computer Engineering

Hitchcock Hall 470
2070 Neil Ave, Columbus, OH 43210
Phone: (614) 292-4282
E-mail: Coifman.1@OSU.edu

Abstract

This paper presents an empirical study of the fundamental relationship between speed, v, and flow, q, (denoted vqFR) under low flow in the uncongested regime. Using new analytical techniques to extract more information from loop detector data, the vqFR from a time of day HOV lane exhibits high v that slowly drops as q increases. This curve arises after binning several million vehicles by q and only considering those bins with q < 1200 vph. A surprising thing happens when further binning the data by the adjacent lane speed (v2): the vqFR expands in to a fan of curves that decrease in magnitude and slope with decreasing v2. Yet each curve in the fan continues to exhibit uncongested trends, ranging from a flat curve consistent with recent editions of the Highway Capacity Manual to downward sloping curves. It is shown that this behavior was not due to the HOV operations per se, the same behavior also arises in the non-HOV period when the lane serves all vehicles and it is also observed at another facility without any HOV restrictions. This dependency on the adjacent lane is absent from most traffic flow theories.

Taking a broader view, four different factors appear to limit the speed a driver takes: (i) the roadway geometry, (ii) the posted speed limit, (iii) the vehicle ahead (car following), and (iv) traffic conditions in the adjacent lane. Whichever constraint is most binding determines the driver's speed. While the first three constraints are found in the literature, this work contributes the fourth, as per above. When the speed limit is the most binding constraint the uncongested regime of the vqFR is roughly flat with a near constant speed over a wide range of q. When the roadway geometry is the binding constraint, e.g., due to the lack of speed limits, drivers are able to travel fast enough to be sensitive to the vehicle ahead and exhibit lower v as q increases. Car following is by definition in the congested regime and thus, beyond the scope of this paper. Finally, the present work shows that as the adjacent lane moves slower, the uncongested drivers choose speeds below the speed limit and once more exhibit lower v as q increases. Although the chosen v is below the speed limit, the drivers continue to exhibit behavior consistent with the uncongested regime.

Keywords

Traffic flow theory, fundamental relationship, flow-density relationship, loop detectors, highway traffic, HOV operations

Highlights

- HOV lane exhibit lower speed at a given flow throughout the uncongested regime
- Results show that this difference is not due to HOV operations per se
- Speed is constant over a range of flow when the adjacent lane is at free speed
- Speed drops as flow increases when the adjacent lane is slow moving
- This dependence on adjacent lanes is absent from most traffic flow theories

1. Introduction

This paper presents an empirical study of the fundamental relationship (FR) between speed, v, and flow, q.[1] For brevity, we refer to this relationship as vqFR. The focus of the study is the uncongested regime of the vqFR under low flow conditions. Before proceeding, it is necessary to briefly review the conventional understanding of the vqFR and its two regimes. The vqFR is characterized as exhibiting an uncongested regime where drivers are free to choose their own speed that is roughly independent of the spacing to the leading vehicle in the same lane; thus, v is near free speed (v_f) as q increases from 0 vph. When q approaches its maximum value at capacity (q_o) then v starts to drop. Within the uncongested regime v is commonly accepted to be either constant yielding a flat curve throughout most of the uncongested regime (e.g., Fig. 1a), or v decreases as q increases yielding a negative slope in the vqFR curve throughout the uncongested regime (e.g., Fig. 1b). Then as v drops below its value at capacity drivers become constrained by their leaders and are no longer free to choose their own speed; thus, the traffic state enters the congested regime, with much lower v, and q now decreasing as v decreases (a positive slope in the vqFR plane, as evident in the lower portion of both plots in Fig. 1).

Using new analytical techniques to extract more information from loop detector data, this paper finds that the empirical vqFR from an active HOV lane exhibits high v that slowly drops as q increases. A surprising thing happens when further binning the data by the adjacent general purpose lane's speed (v2), the HOV lane's vqFR expands into a fan of curves that decrease in magnitude and slope with decreasing v2. Yet each curve in the fan continues to exhibit uncongested trends. It will be shown that this behavior was not due to the HOV operations per se. This location only has a time-of-day HOV restriction and the behavior arises in this same lane when the HOV restriction is inactive. The behavior is also observed on another freeway without any HOV restrictions at a lane drop. The process of identifying the source of this unexpected behavior provides important insights in to the factors that influence a driver's choice of speed in general, and the shape of the vqFR in particular. As discussed herein, it appears that the uncongested vqFR has an intrinsic shape and scale that are determined by various bounding factors, including the speed limit, the roadway design, and this newly found dependency on the adjacent lane speed.

This study is important because the vqFR (and other forms of the FR) are critical for much of traffic flow theory and aspects of traffic operations. A deeper understanding of the factors that influence the shape of the FR will only serve to advance those areas of traffic flow theory and traffic operations that depend on the FR. The FR dates back to Greenshields (1935), who undertook an empirical photographic study of traffic, tabulating speed, v, as a function of flow, q, in what would become known as the fundamental diagram and what the current work calls the vqFR. Greenshields also used dimensional analysis to derive q = kv and project his measurements to density, k. Wardrop (1952) took a more analytical approach to the FR exhibited in the fundamental diagram, providing a rigorous theory of how speed, flow, and density relate. Starting with Lighthill and Whitham (1955) and Richards (1956) the FR became the cornerstone of most traffic flow models. The vqFR is also prevalent in practice for quantifying the level of service (LOS) on highways (see, e.g., the Highway Capacity Manual, TRB, 2000).

[1] The FR relates speed, flow, and density. The relationship is typically presented in the context of two of these three metrics; however, the third metric can easily be calculated from the other two.

1.1. Overview

The remainder of this paper is as follows: Section 2 gives context for this work, both in terms of FR in general, and past studies of inter-lane dependences in the FR in particular. Section 3 presents the analysis, starting with a description of the data and data processing. The section then proceeds to analyze empirical data from two different freeway segments, showing the dependency on the adjacent lanes. The paper closes in Section 4 with a discussion and conclusions.

2. Background

In spite of the importance of the FR, few agree on a single shape or form to the underlying curve. Since the first empirical FR study (Greenshields, 1935) the shape and interpretation of empirical FR curves has evolved over the years. Some of the evolution is due to improvements in transportation infrastructure, the vehicle fleet, and driver capabilities. There have also been changes in data collection methods. Some papers found that the shape of the uncongested regime of the FR to be dependent on the location of data collection (e.g., Hsu and Banks, 1993; Hall et al., 1993; Carter et al., 1999), while others argue that the shape of the FR depends on whether the FR is for individual lanes or for the whole roadway (e.g., Mahabir, 1981; Allen et al., 1985; Ringert and Urbanik, 1993; Hurdle et al., 1997; Carter et al., 1999), and still other papers found a dependency on weather conditions (e.g., Ibrahim and Hall, 1994).

Ultimately, the divergent beliefs of the shape of the FR persist to this day because the empirical data used to study the relationships are quite noisy due to inhomogeneous vehicles, a range of driving behavior, measurement errors, and other factors (Coifman, 2014a). So empirical studies of the FR typically fit a curve to a scattered cloud of points and there is no universally accepted "best fit." The research community has come to accept a blurry picture as a sufficient approximation of a presumed underlying relationship. Unfortunately, this blurred picture obscures critical factors that influence traffic flow.

Among the features lost in the blurry FR are the influences of secondary factors on the shape of the uncongested regime. Some of these factors have been known for years, e.g., the early editions of the Highway Capacity Manual (HCM) suggest that uncongested regime of the vqFR is characterized by speed dropping as flow increases from zero (negative slope throughout the uncongested regime, e.g., Fig. 1b, and as found in HRB, 1950; HRB, 1965; TRB, 1985). More recent literature suggests that the speeds should be roughly constant in the uncongested regime of the vqFR until flow reaches 1,200 vphpl or more (e.g., Fig. 1a, and as found in the 1994 HCM onward; TRB, 1994). Even the explanation of this apparent contradiction is far from new, the 1965 HCM speculated that the negative slope reflected the drivers' innate response to the roadway geometry- taking a precautionary lower speed as the number of ambient vehicles increases- while a flatter vqFR arises in response to speed limits becoming more restrictive than the roadway geometry on driver behavior (HRB, 1965). Although this notion of the speed limit being the most binding constraint is often overlooked, it has been rediscovered several times (e.g., Hall and Brilon, 1994; Hurdle et al., 1997; Bertini et al., 2006a, 2006b).

Coifman (2014a) showed that considerable noise in empirical traffic data comes from the conventional sampling process, whereby vehicles are grouped simply by arrival order over a fixed time period and then their individual measurements are aggregated together to report the average measurement for that sample period. The conventional approach suffers from combining inhomogeneous vehicles together, inclusion of incomplete headways at the start and end of the

sample, and simply a small number of vehicles per sample. In an effort to reduce the noise in empirical traffic detector data, Coifman (2014b) developed the single vehicle passage (svp) method. That work focuses on the congested regime and throughout the congested regime vehicles are binned by length and speed (providing homogeneous vehicles in each bin), samples are exactly one headway (avoiding partial headways by definition), and the results in a given bin are only kept if there are at least 100 observations (ensuring a large number of vehicles per bin). From those bins that remain the median traffic state is calculated (q, v, and occupancy), eliminating the impact of atypical drivers and leading to very clean FR curves across the bins. By virtue of the homogeneous samples, Coifman (2015) showed that the svp can also be used to calculate density and spacing from occupancy.

In Ponnu and Coifman (2015) we extended the svp to study the impact of relative speed to the adjacent lane in the congested regime and found that the vehicles display a conservative behavior, taking a larger spacing for a given speed as the adjacent lane becomes slower. While undertaking the analysis of low flow congested conditions we observed an unexpected behavior in a time-of-day HOV lane. Specifically, there were many slow-moving drivers in the HOV lane that were exhibiting a very large spacing that appeared to be independent of the speed. If the spacings were accurate, they were far too large for these drivers to be car-following and these large spacing drivers appeared to be exhibiting uncongested driving behavior in the context of their own lane. It was not possible to study the vehicles with large spacing using the original svp method that bins vehicles by speed, since these large spacing vehicles would be grouped with the far more dominant number of vehicles that were car following. Although these large spacing vehicles were numerous enough to catch our attention, they still only represented a small minority of the vehicles in a given speed bin and were filtered out when taking the median of the bin. A second factor also precludes the use of speed bins to study the large spacing vehicles since the spacing calculation assumes that successive vehicles roughly maintain their speed after passing the loop detectors. While that assumption might be sufficiently accurate for 1-2 sec, several of the vehicles had headways in excess of 5 sec, increasing the possibility of large changes in speed downstream of the detector and the possibility of lane change maneuvers that would disrupt the relationship.

The research presented in this paper originally set out to investigate the seemingly uncongested slow moving vehicles seen in traffic that was otherwise operating in the congested regime and ultimately found important dependencies in traffic that are absent from conventional traffic flow theory. This in-depth study revealed that these large spacing vehicles did not come from congested regime, instead, they came from the uncongested regime and had unexpectedly low speeds. Thus, the low speed uncongested regime vehicles were grouped by the svp method with a much larger number of congested regime vehicles that fell in the same speed bin. The fact that a given speed corresponds to two different values of flow violates the commonly accepted form of the vqFR, where almost all values of flow correspond to two different v, but all values of speed below free speed should only correspond to a single value of q.[2] As will be discussed in Section 3, it turns out that the multiple values of q for a given v in the vqFR plane arise in response to dependencies on the adjacent lane. Before getting in to the details of the

[2] More sophisticated models may consider the vqFR to be a function of time and location, which can be used to overcome the contradiction, and in general such an approach is likely to be more accurate than assuming a static vqFR curve; however, (i) such models typically offer little guidance as to how the vqFR actually changes over time and space, and (ii), in conventional practice the vqFR is typically considered to be static during the period of interest, e.g., as used in the HCM.

methodology, it is first necessary to place the work in the context of the existing literature that considers inter-lane dependencies, as follows in Section 2.1.

2.1. Literature Review: inter-lane dependencies

There are a few papers that considered adjacent lane impacts while building speed models from a macroscopic perspective. Shankar and Mannering (1998) used loop detector data from I-90 near Seattle aggregated into 1 hr intervals and developed regression models that expressed speed in a lane as a function of the in-lane flow, truck percentage, speed in the adjacent lanes, and many other variables such as the lane-use distribution and a time-of-day indicator. They found that the adjacent lane speed is a statistically significant variable in explaining the in-lane speed. They also developed models for speed deviations in a lane and found that the speed deviation in the adjacent lanes was a significant variable. Himes and Donnell (2010) took a similar approach, except that they used data aggregated at 30-min collected from five roadways in North Carolina and Pennsylvania. Each of the roadways considered in the study had two lanes in each direction and an at-grade and/or a signalized intersection. The authors considered only passenger cars in their analysis as the roadways considered in the work had few heavy vehicles. They also found that both speed and the speed deviation in the adjacent lanes are statistically significant variables in explaining the in-lane speed. A few other papers considered adjacent lane impacts in terms of interaction between flows or densities in the adjacent lane. Gazis et al. (1962) developed a theoretical model to describe density oscillations between two adjacent highway lanes at a macroscopic level, hypothesizing that drivers prefer to avoid being in the slow-moving lane and that the speeds between two adjacent lanes interact through the corresponding densities.

Some papers considered the impact of adjacent lanes in terms of the area surrounding the subject vehicle from a microscopic perspective. Berthaume et al. (2014) proposed a conceptual framework using Lewin's field theory (Lewin, 1936) that considers the impact of the driver's visual area on driver behavior that is not necessarily restricted to the driver's own lane. Mahalel (1984) collected traffic data including: volume, headways and speeds at three rural 4-lane divided highways (2 lanes in each direction) from time-lapse photography. Using these empirical data as inputs, Mahalel developed simulation models to evaluate the longitudinal friction (on the same lane) and lateral friction (across two adjacent lanes) by counting the points at which the vehicle trajectories would potentially intersect given the traffic conditions on the road. He found that both longitudinal and latitudinal friction increase with traffic volumes and the standard deviation of speed. He also found that the interdependence in the arrival between two lanes adjacent to each other increased the latitudinal friction between those two lanes.

As noted previously, empirical vqFR data are typically so noisy that subtle trends cannot be isolated or even identified (e.g., a dependency on the adjacent lane speed). However, there are some facilities that exhibit impacts strong enough that inter-lane dependencies do become evident in the presence of the noisy data. Specifically, high occupancy vehicle (HOV) lanes are intended to maintain a large speed differential between the priority lane and the adjacent general purpose (GP) lanes. As a result, HOV lanes typically exhibit markedly different behavior than GP lanes in empirical FR studies. For example, Guin et al. (2008) found a *sympathetic speed reduction* in the HOV lane due to congestion in the adjacent lane, whereby the drivers in the HOV choose speeds below the speed limit when the GP lane is congested even though the HOV lane is uncongested. Thomson et al. (2012) studied five different types of HOV facilities, namely: continuous single lane, buffer single lane, buffer multiple lane, barrier single lane and

barrier multiple lane. They found that the vqFR on these facilities are affected by the friction effect arising from the congested GP lanes. To account for the friction effect, they developed two different vqFR curves for the HOV lane for (i) GP density < 35 pcpmpl and (ii) GP density > 35 pcpmpl. They also found that in the *buffer with single lane* facilities where overtaking is not permitted, the speed-flow relationships tend to exhibit a negative slope starting from zero flows and they attributed this slope to fast vehicles getting caught behind slower moving vehicles in the HOV lane. In contrast, *continuous lane with passing* and *buffer multiple lane* facilities the free flow speeds remained constant until around 800 vph, which was attributed to drivers being able to pass slower moving vehicles in the HOV lane. Liu et al. (2011) studied four types of facilities, namely: dual HOV lanes with a concrete barrier, single HOV lanes with a soft barrier, single HOV lane with buffer separation, and dual HOV lanes with a buffer. They found that the friction effect of GP lanes on the HOV lanes varied as a function of separation type, GP lane operating speed, and the number of HOV lanes. The separation type had the greatest impact on the friction, with the concrete barrier producing the least friction, followed by soft barrier, and then by buffer separated. They also found that when there were dual HOV lanes in the facility, the friction on the HOV lanes was lower than when there was only a single HOV lane, and like Thomson et al., this finding was attributed to drivers being able to pass slower moving vehicles in the HOV lane. Subsequently, Liu et al. (2012) reported that the vqFR of a buffer-separated HOV lane with adjacent GP lane density greater than 35 pcpmpl lies below the vqFR when the density is less than 35 pcpmpl. Jang et al. (2012) using 5-min aggregated data with density estimated from k = q/v and found that the flow-density relationship of a continuous HOV lane is a function of the relative speed to the adjacent lane. Specifically, they found that the HOV lane speed at a given density increases as the adjacent lane speed increases. Unfortunately, as discussed in Coifman (2014a), density and the arising FR depend on vehicle length, while Coifman (2015) showed that the use of the fundamental equation on data from inhomogeneous vehicles simply masks the length dependency, thus, limiting the accuracy of studies like Jang et al. that use that technique.

Collectively, the HOV papers were inspirational for our study. However, these earlier studies were limited to the resolution and fidelity of conventionally aggregated traffic data. Thus, they were only able to establish the relationships under the extreme speed differentials found in HOV facilities. As a result, (i) they focused strictly on how the HOV lanes differed from GP lanes; (ii) they only lead to very coarse findings, e.g., choosing between one of two vqFR curves in Thomson et al. (2012) and Liu et al. (2012); and (iii) they could not study control conditions on non-HOV facilities.

3. Analysis

3.1. Data Description

The individual vehicle actuations necessary for the svp method are generated at most loop detector stations, but these data typically are not retained, instead, operating agencies aggregate these data in the field to find average speed, flow and occupancy, which are transmitted to a traffic management center and the individual vehicle actuations are discarded in the aggregation process. This paper uses data from two facilities that are exceptions to the rule and at the time of data collection, preserved the individual vehicle actuations. The first location is the Berkeley Highway Laboratory (BHL) (Coifman, et al., 2000). The BHL data used in this study is the data set from Ponnu and Coifman (2015), and the present work only uses those data

from the two left-most lanes. These data come from a roughly 2 mile long stretch of eastbound I-80 in Emeryville and Berkeley, California. The freeway has 5 lanes, numbered from the inside (median) lane 1, to the outside (shoulder) lane 5. Lane 1 is a time of day HOV lane that reverts to general purpose (GP) outside of the period of HOV operations. The only distinction that drivers see of lane 1 is diamond markings on the pavement and signage along the right of way. The width of lane 1 and striping between lanes 1 and 2 is otherwise identical to that of the GP lanes. The data come from 69 weekdays in September through December in 1999 from dual loop detector stations 1, 2, 3, 4 and 6 in the BHL while the remaining weekdays were excluded due to either incidents or public holidays. Station 5 data were not used as one of the two dual loop detectors in the HOV lane was not operational during the time period of study. The speed limit at the time of collection was 65 mph. This study uses two different time windows for the I-80 data around the evening peak period, the first is while the HOV restriction is active, termed "HOV period", between 15-19 hours. The second is when lane 1 serves as a GP lane, termed "non-HOV period" during 13-14.75 and 19.25-21 hours. Trucks are restricted from lanes 1 and 2, though somewhat frequent buses and an occasional violating truck can be seen in these lanes.

The second data set comes from the Columbus Metropolitan Freeway Management System (CMFMS) (Coifman et al., 2015). The data used in this study comes from station 1 northbound on I-71 in Columbus, Ohio. In contrast to I-80, this freeway does not have any HOV lanes. There are four lanes at this location on I-71 (numbered from lane 1 on the inside to lane 4 on the outside) and it is situated a little over a half mile upstream of a lane drop where lane 4 drivers must merge into lane 3. There are no intervening ramps between the detector station and the lane drop. This research uses data from 172 weekdays in 2007 at this station. The speed limit at the time of collection was 65 mph.

3.1.1. The Single Vehicle Passage Method

This paper uses a modified version of the svp methodology proposed by Coifman (2014b) and extended in Ponnu and Coifman (2015). The svp method greatly improves the fidelity of loop detector data by eliminating many confounding factors (e.g., inhomogeneous vehicles, truncated headways, and small number of vehicles per bin) and allowing one to isolate features of interest (e.g., the adjacent lane speed). The svp method entails the processing of individual vehicle actuation data from dual loop detectors. Reiterating the process here for easy reference, first for each single vehicle passage, the flow q_{svp}, occupancy occ_{svp}, speed v_{svp} and length L_{svp} are calculated via Equations 1-4. Where h is the headway of the vehicle measured rear bumper of the previous vehicle to the rear bumper of the current vehicle to ensure that the gap ahead of the current vehicle is associated with that vehicle. On-time is the time for which the vehicle occupied the upstream detector, detector spacing is the distance between the two loops of the dual loop detector. The traversal time is the time of travel of the vehicle between the rising edges of the vehicle actuation at the upstream and the downstream detectors.

$$q_{svp} = \frac{1}{h} \tag{1}$$

$$occ_{svp} = \frac{on\_time}{h} * 100\% \tag{2}$$

$$v_{svp} = \frac{detector\_spacing}{traversal\_time} \tag{3}$$

$$L_{svp} = v_{svp} * on\_time \tag{4}$$

Coifman (2014b) sampled over 1.2 million svp measurements from a freeway and binned them by length and vehicle speed, with a focus on the vehicles in the congested regime. The length bins spanned 5 to 10 ft and the speed bins spanned 1 mph. Within each bin if there were at least 100 observations the median traffic state was found (where the traffic state is given by Equations 1-4) and used in the analysis, while bins with fewer than 100 observations were excluded from further consideration. The primary focus in that paper was speed bins between 5 and 17 mph, but the results included the span of speed bins from 1 to 50 mph. Ponnu and Coifman (2015) extended the svp methodology to also bin by relative speed to the adjacent lane. With the additional dimension that research had to sample more vehicles (over 4.8 million svp measurements in the study lane) and only focused on the most dominant length bin, namely passenger vehicles with effective length between 18 and 22 ft (the passenger vehicles make up over 70% of the observations in the lanes of study).

3.1.2. Data aggregation

As noted in Section 2, Ponnu and Coifman (2015) focused strictly on the congested regime, where speed and spacing are highly correlated, hence the use of speed bins in that paper. The present study focuses on low flow within the uncongested regime, where speed and spacing should have little correlation. Within the low flow portion of the uncongested regime, conventional theory dictates that drivers generally have more than enough spacing, so they can simply choose to drive at their preferred speed with little or no influence from their leader. Hence, this work modifies the svp to bin by flow rather than speed, using 50 vph bins to balance step size and sample size. The maximum flow considered in the study is 1200 vph which corresponds to a minimum headway of 3 sec.

One drawback of binning by flow is the fact that each value of flow on a vqFR curve should correspond to one speed in the uncongested regime and another speed much lower in the congested regime. When looking at the underlying raw data there is not even a single curve, rather, a bimodal distribution of speeds within a given flow bin. Fig. 2a-c shows the histogram of the number of vehicles at a given speed, v1, as seen in a given flow bin, q1, for the subject lane. The three plots show the same region of the vqFR plane, as binned by different ranges of the adjacent lane speed, v2 (note that the peak number of samples on the vertical axis increases by roughly a factor of three from one plot to the next). To facilitate interpretation of the plots, Fig. 2d-f repeat the histograms in 2 dimensions, using shading to denote the percentage of vehicles. For the lowest v2 bin (0-10 mph) Fig. 2d shows data in both the uncongested regime: v1 between 30 and 60 mph, with a slightly negative slope, and congested regime: v1 between 0 and 20 mph, with a positive slope. Throughout the range of q1 (0-1200 vph) there is a clear division between the modes corresponding to the two regimes in this subplot. Meanwhile, in the higher v2 bins, Fig. 2e-f show little or no evidence of any data coming from the congested regime. So, all vehicles in the subject lane with speed below 20 mph are excluded from further analysis, as these vehicles clearly come from the congested regime.

The present work also differs from Ponnu and Coifman (2015) in a few more important ways. First, instead of binning by relative speed between the two lanes, v12, the present work bins simply by the adjacent lane speed, v2. The use of relative speed as was done in the earlier paper was not a problem there since vehicles were already binned by v1. Now, however, v2 ranges from 0 to 80 mph while v1 ranges from 40 to 80 mph. The use of relative speed restricts the range of v1 since v12 = v1 - v2, and as a result, the use of v12 would still effectively bin the data by v1, and binning by v1 is something that we specifically want avoid in this work that already bins by q1.

Second, instead of finding the median of a given bin, this paper uses the harmonic mean speed of all vehicles in a given bin (i.e., after binning by length, q1, and where applicable, after binning by, v2). While the median remains attractive in terms of its insensitivity to outliers, it proves disadvantageous with the high speeds in the uncongested regime. The dual loop detectors are sampled at 60 Hz and the paired loops are 20 ft apart. As a result, for speeds above 50 mph there are very pronounced steps between resolvable speeds, e.g., between 55 mph and 80 mph the only resolvable speeds are 58.4, 62.9, 68.2 and 74.4 mph. These resolvable steps are far too coarse to clearly see the features of interest. We analyzed the data using: (i) median speed of each bin, (ii) harmonic mean of each bin after excluding all v1 < 20 mph, and (iii) arithmetic mean of each bin including all v1. The general results were similar across all three approaches, but approach i suffered from poor resolution due to the coarse step size between resolvable speeds, and approach iii was more sensitive to occasional measurement errors that result in an unreasonably high individual speed measurements (e.g., the next three faster resolvable bins are 81.2, 90.1, and 102.3 mph, so a sampling error of 1/60 sec could result in a 10 mph measurement error).

In summary, the lane 1 vehicles were (1) binned by length, and only the 18-22 ft vehicles were retained, (2) binned by q1 in to 50 vph bins and only q1 ≤ 1200 vph were retained, and (3) binned by v2 in 10 mph bins. At this point any v1 < 20 mph was discarded as those vehicles came from the congested regime.[3] Any individual bin with fewer than 100 vehicles was discarded. Finally, the harmonic mean speed was found for all vehicles in a given bin. After all of this processing just over 289,000 vehicle actuations in lane 1 on I-80 met the binning criteria for the HOV period, and another 266,000 vehicle actuations in lane 1 for the non-HOV period.

3.2. Application

Fig. 3a shows the harmonic speed in each flow bin from lane 1 at each station during the HOV period without binning by v2. These empirical vqFR curves exhibit a nearly constant negative slope as speeds drop from around 60 mph at 135 vph. Fig. 3b repeats the analysis for the non-HOV period. Compared to Fig. 3a, the speeds are higher for a given q in the vqFR curves. At low flows the slope is flatter than during the HOV period and slowly becomes more negative as flow increases. In either case, all of the stations exhibit similar trends. Fig. 3c combines the data across all of the stations, showing the HOV and non-HOV periods as separate vqFR curves on the same plot. There is clearly a different magnitude and slope to the uncongested vqFR in the two different time periods. For reference, Fig. 3d-f repeat the analysis using the arithmetic mean and no lower bound on v1 in the given bin, illustrating the similar results using different measures of the central tendency.

Returning to the harmonic mean and now binning by v2, Fig. 4a-e show the resulting vqFR for the data from each of the five stations for the HOV period and all five stations combined in Fig. 4f. Each station shows a fan of curves, with both the slope and the magnitude of the uncongested regime of the vqFR in lane 1 strictly decreasing as v2 decreases (with the highest v2 bin being roughly zero slope). Thus, the curve for each successive v2 bin falls strictly below that of the preceding v2 bin, with 60-70 mph at the top in each plot and 0-10 mph at the bottom. For reference, the two curves without v2 bins from Fig. 3c are repeated in each of the plots. It is clear that the highest v2 bin is more like the non-HOV collective curve ("+" symbols)

[3] The analysis was repeated with the arithmetic mean and no lower bound on v1. Except for a brief example in the next section the results from the arithmetic mean are not shown in this paper; however, the resulting trends were similar to the figures and tables in this paper.

than the HOV collective curve ("o" symbols). But only a minority of v2 fall in this bin, and the HOV collective curve falls close to that of the v2 40-50 mph bin at low q1 and the v2 30-40 mph bin at higher q1, suggesting that as v2 drops that v1 drops and q1 rises. It is also worth noting the range of headways, h1, captured in this figure. The secondary horizontal axis in all of the plots show that the vehicles in the flow bins exhibited headways from 3 to 15 sec,[4] and even with 15 sec headways the impact of the adjacent lane is still evident as v1 decreases with v2.

Fig. 5 repeats the analysis for the non-HOV period. Now there are far fewer v2 bins, and those that are populated exhibit generally higher v1 and flatter curves than seen in the HOV period for the same v2. Still, the curve for each successive v2 bin falls strictly below that of the preceding v2 bin, now with 70-80 mph at the top. This fan of curves during the non-HOV period shows that the impact of v2 is not simply due to the HOV operations per se. Even when lane 2 is freely flowing and lane 1 is serving general purpose vehicles, on average the lane 1 drivers slow in response to lower v2. The far greater range of impacts of v2 on v1 seen in the HOV period is simply due to the fact that the HOV restriction allows v1 to remain in the uncongested regime while v2 is considerably lower in the congested regime. This finding is in contrast to the conclusions of Gazis et al. (1962) that found the densities of two adjacent lanes interact with each other due to drivers' desire to be in the fast-moving lane. While it is quite likely that drivers in adjacent lanes harmonize speed via lane change maneuvers to get into the fast-moving lane, Figs. 4-5 show that there is another mechanism at work, whereby drivers in a fast-moving lane naturally slowdown in response to slower traffic in the adjacent lane.

The range of curves seen in Figs. 4-5 is also remarkable: when v2 is high, the uncongested lane 1 vqFR is virtually flat between 0 and 1200 vph, similar to recent editions of the HCM (TRB, 2000). But when v2 is low, the slope of the vqFR is negative throughout the same q1 range, similar to older HCM (TRB, 1985).

3.2.1. Analysis using I-71 svp data- traffic at a non-HOV facility

Now moving to the CMFMS data on I-71, this section uses station 1 northbound situated a little over a half mile upstream of a lane drop where lane 4 drivers must merge into lane 3. There are no intervening ramps between the detector station and the lane drop. As such, during uncongested conditions there is little incentive to travel in lane 4 and typically lane 4 flows, q4, increase as lanes 1-3 become increasingly congested. In this shift to I-71 it is first necessary to revise the length bin. While the dominant effective vehicle length range in I-80 was from 18-22 ft (i.e., due to passenger cars), on I-71 this range shifts to 20.55-24.55 ft due to higher detector sensitivity at this station. It was also necessary to explicitly define the peak and non-peak periods that were previously set to the time of day HOV start and end times on I-80. As observed from the time series of speeds at this station for the 172 days considered in the dataset, the daily peak traffic volume at the station occurs between 15-19 hours and outside of this time period the station is generally uncongested during the rest of the day. After all of this processing just over 86,000 vehicle actuations in lane 4 met the binning criteria for the peak period (15-19 hrs), and another 110,000 vehicle actuations in lane 4 for the non-peak period (limited to 6-15 and 19-22 hrs to avoid exceptionally low flow during the early morning).

Fig. 6a shows the resulting vqFR during the peak period of 15-19 hrs. Once more the fan of curves emerges with the magnitude and slope being functions of the adjacent lane speed. Like the HOV facility on I-80, the highest adjacent lane speed bin (v3 in this case) is the top curve in

[4] Recall from Equation 1 that $q_{svp} = 1/h$, so the headways in this plot are the true individual headways observed rather than an average of widely disparate headways.

the plot, and each successive v3 bin moves to the next lower curve. While the large difference between adjacent lane speeds on I-80 arose from the HOV restriction, here the discrepancy arises from the fact that the subject lane ends and thus, the mandatory lane change maneuver creates a disincentive to be in lane 4 when all other things are equal. Presumably for the drivers the benefit of the higher v4 is at equilibrium with the extra cost of making the subsequent lane change maneuver. In any event, this plot clearly shows that the phenomenon transcends HOV facilities. Compared to Fig. 4f both the magnitude and slopes are smaller for a given adjacent lane speed, but the speed limit, number of lanes, population of drivers, etc. differ between the two facilities. Finally, Fig. 6b shows the results on I-71 for the non-peak period. Like I-80, the range of speeds is smaller than the peak period, but the dependency on the adjacent lane remains with the vqFR curve for each successive v3 bin falling below the curve from the next higher v3 bin.

3.3. Fitting Regression Models to the vqFR Curves

Linear regression models were fit to the vqFR curves binned by adjacent lane speed (v2) from I-80 in Fig. 4F and 5F. The fitted functions are shown in Fig. 7. The estimated intercepts and slopes from linear regression are shown in Tables 1 and 2 along with the standard error, mean absolute percentage error (MAPE), number of samples, the model F-statistic and the p-value of the F-statistic indicating the validity of the model for each v2 bin in the two different time periods.[5] The p-value indicates that all of the models in Tables 1 and 2 are statistically significant except for the v2 bin of 30-40 mph bin during the non-HOV period (this specific bin has only 4 samples). Excluding the statistically insignificant v2 bin, Tables 1 and 2 show that the slope of the uncongested vqFR curves change from being close to horizontal for the highest v2 bins and then the slope becomes more and more negative as v2 drops for both the HOV and non-HOV time periods. The tables also show that the intercept decreases as v2 decreases. Looking at the computed MAPE values of the models from Tables 1 and 2, it can be seen that all twelve of the models have a MAPE of less than 1% indicating that the models are indeed a good fit to the data.

This process was repeated for vqFR curves binned by adjacent lane speed (v3) for I-71 in Fig. 6. The fitted functions are shown in Fig. 8 and Tables 3 and 4 summarize the results. The p-value indicates that all of the models in Tables 3 and 4 are statistically significant except for the v3 bins of 40-50 mph and 70 to 80 mph during the 6-15 and 19-22 hours (again due at least in part to relatively small sample size in these bins). Excluding the statistically insignificant v3 bins, once more the models exhibit the trend that the slope of the vqFR becomes more and more negative as the adjacent lane gets slower. Further, the standard errors of the fitted models during the two different time periods range from 0.199 to 0.592 mph and the MAPE from 0.24 to 0.86% showing that the fitted models of I-71 perform well and the general trends are similar to the models from I-80.

4. Discussion and Conclusions

This paper used a modified version of the single vehicle passage (svp) method to show that the shape of the uncongested regime of the vqFR in a study lane depends upon traffic

[5] The conventional measure R^2 was not used to assess the goodness of fit of the models as it was found to be penalizing those v2 bin models for which the slope was near horizontal (e.g., 70 to 80 mph v2 bin during the non-HOV hours) even though these near horizontal models were visually comparable to the other models with slopes slightly less than zero. Hence the standard error of the regression model was used to measure how well the model represented the observed data.

conditions in the adjacent lane. This dependency on the adjacent lane is absent from most traffic flow theories. The svp method was critical to revealing these findings, as it greatly improves the fidelity of loop detector data by eliminating many confounding factors (e.g., inhomogeneous vehicles, truncated headways, and small number of vehicles per bin) and allowing one to isolate features of interest (e.g., the adjacent lane speed). The study was limited to the left most and right most lanes in part to exploit traffic dynamics that can sustain a large difference in speed between the study lane and adjacent lane, and in part to avoid having to isolate the impacts of two different adjacent lanes that would be found in the center lanes. Much of the study was focused on a time of day HOV lane on I-80. When the HOV restriction was active, the low flow, uncongested regime of the vqFR showed a clear dependency on the adjacent lane. While the study lane exhibited behavior consistent with the uncongested regime throughout the range of the adjacent lane speeds (e.g., a constant or negative slope), the slope and magnitude of the vqFR both decreased as the adjacent lane speed decreased, e.g., Fig. 4. Based on this evidence alone, one might be tempted to attribute root cause of this behavior to the HOV operations, e.g., perhaps there was insufficient demand in the HOV lane to achieve some desired flow and so the vqFR was stunted in the dimension of flow. However, this supposition is where the time of day HOV restriction is important. Outside of the HOV period the study lane serves general purpose vehicles. It was shown that the vqFR dependency on the adjacent lane speed persisted during the non-HOV period, albeit with a much smaller dynamic range since single occupant vehicles could switch between lanes at will with the byproduct of limiting just how low the adjacent lane speed could drop without pulling the study lane speed with it, e.g., Fig. 5. The analysis was then repeated on a lane drop on I-71, where the study lane ended within a half mile downstream of the detector station used. At this site, there was no HOV lane. Instead, the presence of the lane drop was a disincentive to be in the study lane, thus, providing a different mechanism to sustain a large difference in speed between the study lane and adjacent lane. Here too, the uncongested regime of the vqFR exhibited a dependency on the adjacent lane similar to that seen on the HOV facility, e.g., Fig. 6.

These findings provide important insights in to the factors that influence a driver's choice of speed. Specifically, there appears to be four different factors that limit the speed a driver takes: (i) the roadway geometry, (ii) the posted speed limit, (iii) the vehicle ahead (car following), and (iv) the traffic conditions in the adjacent lane. Whichever constraint is most binding determines the driver's speed. While the first three constraints can be found in the literature, this work contributes the fourth, i.e., the dependency on the adjacent lane. When the speed limit is the most binding constraint the uncongested regime of the vqFR is roughly flat with a near constant speed over a wide range of q. When the roadway geometry is the binding constraint, e.g., due to the lack of speed limits, drivers are able to travel fast enough to be sensitive to the vehicle ahead and exhibit lower v as q increases, thus, the uncongested regime of the vqFR exhibits a negative slope. When drivers are car following, they are by definition in the congested regime and beyond the scope of this work. Finally, the present work shows that as the adjacent lane moves slower, the uncongested drivers in the study lane choose speeds below the speed limit and once more exhibit lower v as q increases. Although the chosen v is below the speed limit, the drivers continue to exhibit behavior consistent with the uncongested regime, i.e., the vqFR exhibits a negative slope in response to the vehicle ahead. This adjacent lane constraint differs from the roadway geometry in that the given vqFR curve changes depending on the adjacent lane speed and when the adjacent lane speed is high enough the vqFR flattens out and the speed limit dominates.

Finally, a word of caution in the use of the results presented herein. The various vqFR developed in this paper clearly demonstrate a dependence on the adjacent lane speed; however, a reader should use discretion in generalizing the specific vqFR curves to mixed traffic. The svp measurements only capture what individual drivers are doing when they are grouped with many similar drivers in terms of vehicle length, adjacent lane speed, and chosen headway (recall that the low flows in this paper correspond to long headways). In normal traffic the adjacent lane speed could span a large range during a conventional 30 sec sample and the adjacent lane speed would almost certainly do so during a conventional 5 min sample from congested conditions. Many different time series of the adjacent lane speed will yield the same conventional aggregate average speed in that lane, so it would be impossible to identify the sequence of adjacent lane speeds seen by the individual vehicles, e.g., on I-80 the traffic state over 5 min will likely jump across many curves in Fig. 4f in a pattern that cannot be identified from the aggregate v2 for the given sample period. The mixture of many inhomogeneous drivers and vehicles will further obscure these relationships, e.g., a conventional 30 sec sample might have a single long headway vehicle (studied herein) and several short headway vehicles (beyond the scope of this paper). Such short headway vehicles are the subject of ongoing research, and while the dependence on the adjacent lane speed persists for those short headway vehicles, the observed vqFR for the short headway vehicles differ from the vqFR curves for the long headway vehicles presented herein.

Acknowledgements

This material is based in part upon work supported in part by the National Science Foundation under Grant No. 1537423 and in part by Ohio State University's Crash Imminent Safety (CrIS) a USDOT Tier I University Transportation Center. The contents of this report reflect the views of the authors who are responsible for the facts and the accuracy of the data presented herein. The contents do not necessarily reflect the official views or policies of the Federal Highway Administration. This report does not constitute a standard, specification or regulation.

References

Allen, B. L., F. L. Hall, and M. A. Gunter. (1985) "Another Look at Identifying Speed–Flow Relationships on Freeways", *Transportation Research Record 1005*, pp. 54–64.

Berthaume, A. L., Romoser, M. R., Collura, J., and Ni, D. (2014) "Towards a Social Psychology-based Microscopic Model of Driver Behavior and Decision making: Modifying Lewin's Field Theory", *Proc. 3rd International Workshop on Agent-based Mobility, Traffic and Transportation Models, Methodologies and Applications*, Procedia Computer Science, Vol. 32, pp. 816- 821.

Bertini, R. L., Boice, S., and Bogenberger, K. (2006a) "Dynamics of Variable Speed Limit System Surrounding Bottleneck on German Autobahn", *Transportation Research Record 1978*, pp. 149–159.

Bertini, R. L., Boice, S., and Bogenberger, K.(2006b) "Comparison of Key Freeway Capacity Parameters on North American Freeways with German Autobahns Equipped with a

Variable Speed Limit System", *Proc., 5th International Symposium on Highway Capacity and Quality of Service,* Yokohama, Japan, 2006.

Carter, M., Rakha, H., Van Aerde, M. (1999) "Variability of Traffic-Flow Measures across Freeway Lanes", *Canadian Journal of Civil Engineering*, Vol. 26, No. 3, pp. 270–281.

Coifman, B., Huang, B., Redmill, K., Wu, M. (2015) *Mining vehicle classifications from the Columbus Metropolitan Freeway Management System*, Ohio Department of Transportation; Federal Highway Administration, 70p

Coifman, B., Lyddy, D., and Skabardonis, A., (2000) "The Berkeley Highway Laboratory-Building on the I-880 Field Experiment," *Proc. IEEE ITS Council Annual Meeting,* IEEE, pp 5-10.

Coifman, B. (2014a) "Jam Occupancy and Other Lingering Problems with Empirical Fundamental Relationships," *Transportation Research Record 2422*, pp. 104-112.

Coifman, B. (2014b) "Revisiting the Empirical Fundamental Relationship", *Transportation Research- Part B*, Vol. 68, pp. 173-184.

Coifman, B. (2015) "Empirical Flow-Density and Speed-Spacing Relationships: Evidence of Vehicle Length Dependency", *Transportation Research- Part B*, Vol. 78, pp. 54-65.

Gazis, D. C., Herman, R., and Weiss, G. H. (1962) "Density Oscillations Between Lanes of a Multilane Highway", *Operations Research*, Vol. 10, No. 5, 658–667.

Greenshields, B. D. (1935), "A Study of Traffic Capacity", *Proc. of 14th Annual Conference of the Highway Research Board*, pp. 448-477.

Guin, A., Hunter, M. P., Guensler, R. L. (2008) "Analysis of Reduction in Effective Capacities of High-Occupancy Vehicle Lanes related to Traffic Behavior", *Transportation Research Record 2065*, pp. 47–53.

Hall, F. L., Brilon, W. (1994) "Comparison of Uncongested Speed-Flow Relationships Using Data from German Autobahns and North American Freeways," *Transportation Research Record 1457*, pp. 35-42.

Hall, F. L., Pushkar,A., Shi. Y. (1993) "Some Observations on Speed-Flow and Flow-Occupancy Relationships under Congested Conditions", *Transportation Research Record 1398,* pp. 24–30.

HRB (1950). *Highway Capacity Manual*, Highway Research Board, Bureau of Public Roads, US Department of Commerce, Washington, D.C.

HRB (1965). *Highway Capacity Manual*, Highway Research Board, Bureau of Public Roads, US Department of Commerce, Washington, D.C.

Himes, S. C., Donnell, E. T. (2010) "Speed Prediction Models for Multilane Highways: Simultaneous Equations Approach", *Journal of Transportation Engineering*, Vol. 136, No.10, pp. 855–862.

Hsu, P., Banks, J.H. (1993) "Effects of Location on Congested-Regime Flow–Concentration Relationships for Freeways", *Transportation Research Record 1398*, pp. 17–23.

Hurdle, V.F., Merlo, M.I., Robertson, D. (1997) “Study of Speed-Flow Relationships on Individual Freeway Lanes”, *Transportation Research Record 1591, pp. 7-13*.

Ibrahim, A.T., Hall, F.L. (1994) “Effect of Adverse Weather Conditions on Speed-Flow-Occupancy Relationships”, *Transportation Research Record 1457*, pp. 184–191.

Jang, K., Oum, S., Chan, C. (2012) “Traffic Characteristics of High-occupancy Vehicle Facilities: Comparison of Contiguous and Buffer-separated Lanes”, *Transportation Research Record 2278*, pp. 180–193.

Lewin, K. (1936), *Principles of Topological Psychology*. New York: McGraw-Hill.

Lighthill, M., Whitham, G. (1955) "On Kinematic Waves II. a Theory of Traffic Flow on Long Crowded Roads, "*Proc. Royal Society of London, Part A*, Vol. 229, No. 1178, pp 317-345.

Liu, X., Schroeder, B., Thomson, T., Wang, Y., Rouphail, N., Yin, Y. (2011) “Analysis of Operational Interactions between Freeway Managed Lanes and Parallel, General Purpose Lanes”, *Transportation Research Record 2262*, pp. 62-73.

Liu, X., Zhang, G., Lao, Y., Wang, Y. (2012) “Modeling Traffic Flow Dynamics on Managed-Lane Facility: Approach Based on Cell Transmission Model”, *Transportation Research Record 2278, pp. 163-170*.

Mahabir G. P. (1981) *Speed, Flow and Capacity Relations on Multilane Highways*, M. Eng. Thesis, Dept. of Civil Engineering, McMaster University, Hamilton, Ontario.

Mahalel, D. (1984) “Appraisal of traffic stream friction”, *Transportation Research - Part A*, Vol. 18, No. 3, pp. 225–230.

Ponnu, B., Coifman, B., (2015) "Speed-Spacing Dependency on Relative Speed from the Adjacent Lane: New Insights for Car Following Models," *Transportation Research-Part B,* Vol. 82, pp. 74–90.

Richards, P., (1956) "Shock Waves on the Highway," *Operations Research*, Vol. 4, No. 1, pp 42-51.

Ringert, J., Urbanik II, T. (1993), “Study of Freeway Bottlenecks in Texas”, *Transportation Research Record 1398*, pp. 31-41.

Shankar, V., and Mannering, F. (1998) “Modeling the endogeneity of lane-mean speeds and lane-speed deviations: a structural equations approach”, *Transportation Research - Part A*, Vol. 32, No. 5, pp. 311–322.

Thomson, T., Liu, X., Wang, Y., Schroeder, B. J., Rouphail, N. M. (2012) “Operational Performance and Speed–Flow Relationships for Basic Managed-Lane Segments”, *Transportation Research Record 2286*, pp. 94-104.

TRB (1985), *Highway Capacity Manual*, Transportation Research Board, National Research Council, Washington, D.C.

TRB (1994), *Highway Capacity Manual*, Transportation Research Board, National Research Council, Washington, D.C.

TRB (2000), *Highway Capacity Manual*, Transportation Research Board, National Research Council, Washington, D.C.

Wardrop, J. 1952, "Some Theoretical Aspects of Road Traffic Research", *Proc. Inst. Civil Engineers*, Part II 1, pp. 325-362.

Table 1, I-80 lane 1 eastbound vqFR linear regression models for 18-22 ft vehicles sorted by v2 bins across all stations combined during the HOV period.

v2 bin, (mph)	Intercept, (mph)	Slope, (mph/vph)	Std. error, (mph)	MAPE, %	# samples	F-stat	p-value
60 to 70	68.530	-0.00049	0.189	0.223	22	14.968	0.001
50 to 60	64.859	-0.00235	0.248	0.281	22	197.697	0.000
40 to 50	59.846	-0.00400	0.248	0.316	22	572.554	0.000
30 to 40	55.644	-0.00519	0.507	0.564	22	229.714	0.000
20 to 30	52.639	-0.00592	0.421	0.565	22	432.140	0.000
10 to 20	50.916	-0.00709	0.489	0.747	21	402.975	0.000
0 to 10	50.178	-0.00853	0.544	0.807	20	406.148	0.000

Table 2, I-80 lane 1 eastbound vqFR linear regression models for 18-22 ft vehicles sorted by v2 bins across all stations combined during the non-HOV period.

v2 bin, (mph)	Intercept, (mph)	Slope, (mph/vph)	Std. error, (mph)	MAPE, %	# samples	F-stat	p-value
70 to 80	71.823	0.00022	0.105	0.117	23	10.560	0.004
60 to 70	71.067	-0.00048	0.079	0.078	23	92.527	0.000
50 to 60	69.376	-0.00311	0.179	0.205	22	658.860	0.000
40 to 50*	59.554	-0.00832	0.483	0.739	11	81.205	0.000
30 to 40*	40.894	-0.00184	0.304	0.456	4	0.425	[0.582]

Notes:

* These v2 bins marked with an asterisk were only observed on days where there was an incident

Text in square brackets indicates that the corresponding models are not statistically significant

Table 3, I-71 lane 4 northbound vqFR linear regression models for 20.6-25.6 ft vehicles sorted by v3 bins during the peak period.

v3 bin, (mph)	Intercept, (mph)	Slope, (mph/vph)	Std. error, (mph)	MAPE	# samples	F-stat	p-value
60 to 70	65.977	-0.00065	0.331	0.383	24	11.019	0.003
50 to 60	63.651	-0.00092	0.251	0.278	24	38.185	0.000
40 to 50	57.887	-0.00238	0.592	0.741	15	11.209	0.005
30 to 40	51.375	-0.00276	0.539	0.841	22	57.568	0.000
20 to 30	45.375	-0.00351	0.452	0.858	23	151.310	0.000
10 to 20	41.489	-0.00466	0.223	0.466	23	1094.353	0.000
0 to 10	39.385	-0.00500	0.531	1.132	23	222.789	0.000

Table 4, I-71 lane 4 northbound vqFR linear regression models for 20.6-25.6 ft vehicles sorted by v3 bins during the non-peak period.

v3 bin, (mph)	Intercept, (mph)	Slope, (mph/vph)	Std. error, (mph)	MAPE	# samples	F-stat	p-value
70 to 80	66.867	0.00077	0.423	0.468	10	0.657	[0.441]
60 to 70	66.225	-0.00059	0.199	0.244	24	25.207	0.000
50 to 60	64.269	-0.00090	0.269	0.330	24	32.090	0.000
40 to 50	59.942	0.00006	0.484	0.672	12	0.005	[0.947]

Notes:

Text in square brackets indicates that the corresponding models are not statistically significant

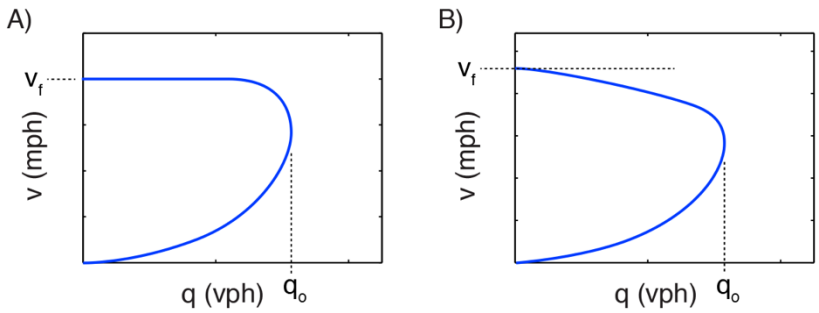

Figure 1, Hypothetical examples of the most commonly accepted shapes of the vqFR, with the uncongested regime at the top and the congested regime at the bottom. Within the uncongested regime, (A) speeds remain nearly constant at v_f as q increases from 0 vph and do not start to drop until q approaches capacity at q_o, yielding a "flat" vqFR curve in the uncongested regime; or (B) speeds drop throughout the uncongested regime as q increases, yielding a negatively sloped vqFR curve in the uncongested regime.

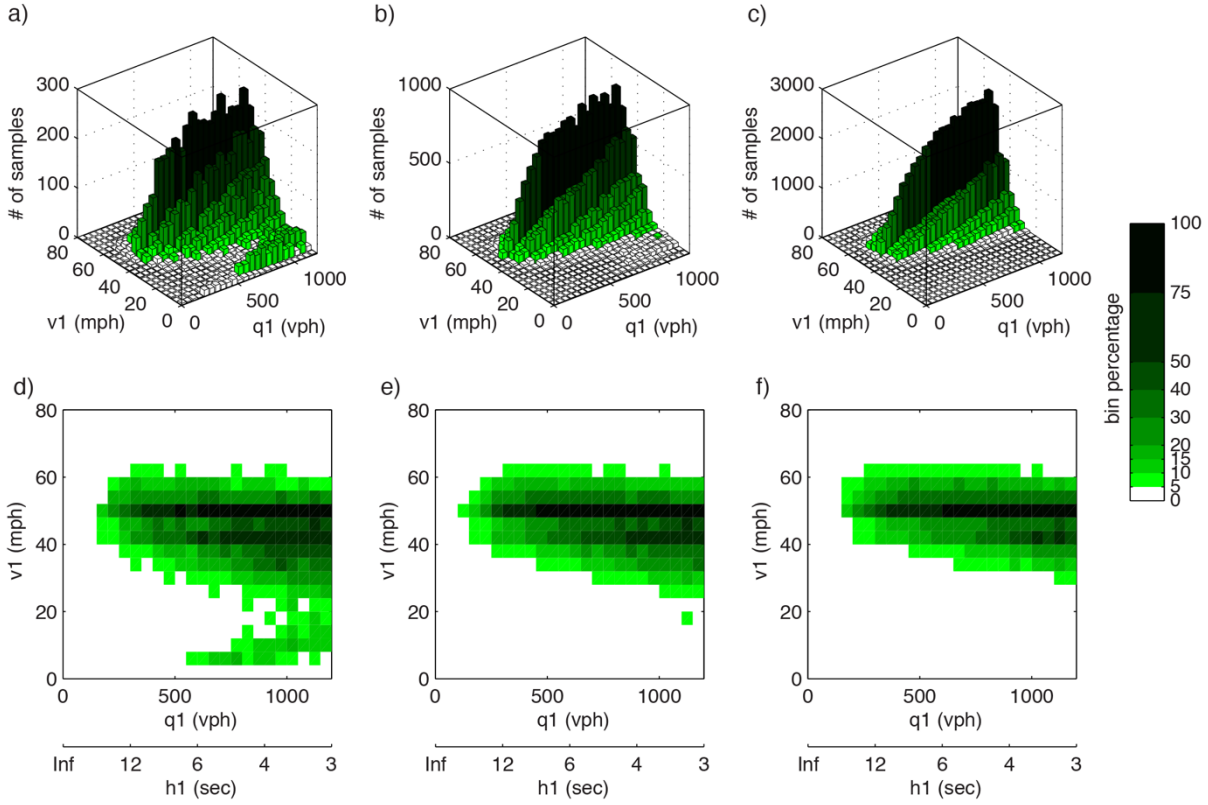

Figure 2, Number of samples and percentage in a given q1 bin for the three lowest v2 bins from I-80 lane 1 eastbound, shown in a 3D histogram for (a) v2 0 to 10 mph, (b) v2 10 to 20 mph, (c) v2 20 to 30 mph. Note that the peak number of samples on the vertical axis increases by roughly 3x from one plot to the next. Repeating the plots in 2D with shading denoting the percentile (d) v2 0 to 10 mph, (e) v2 10 to 20 mph, (f) v2 20 to 30 mph.

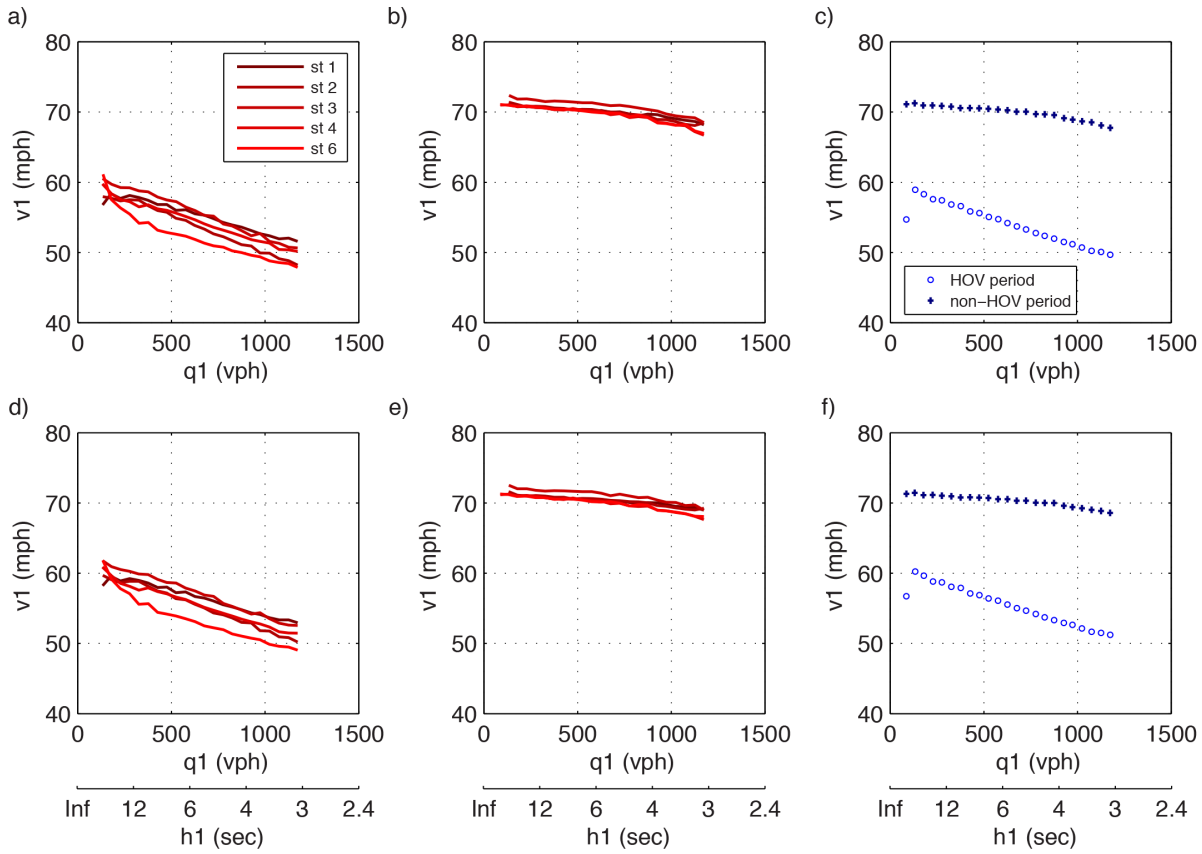

Figure 3, I-80 lane 1 eastbound vqFR plane for 18-22 ft vehicles showing harmonic mean v1 in each q1 bin for each station after excluding v_{svp} < 20 mph, (a) HOV period, and (b) non-HOV period. (c) Repeating the harmonic mean v1 only now combining all stations together and plotting the respective curve for each time period. (d-f) Repeating the plots only now using the arithmetic mean and including all v_{svp}.

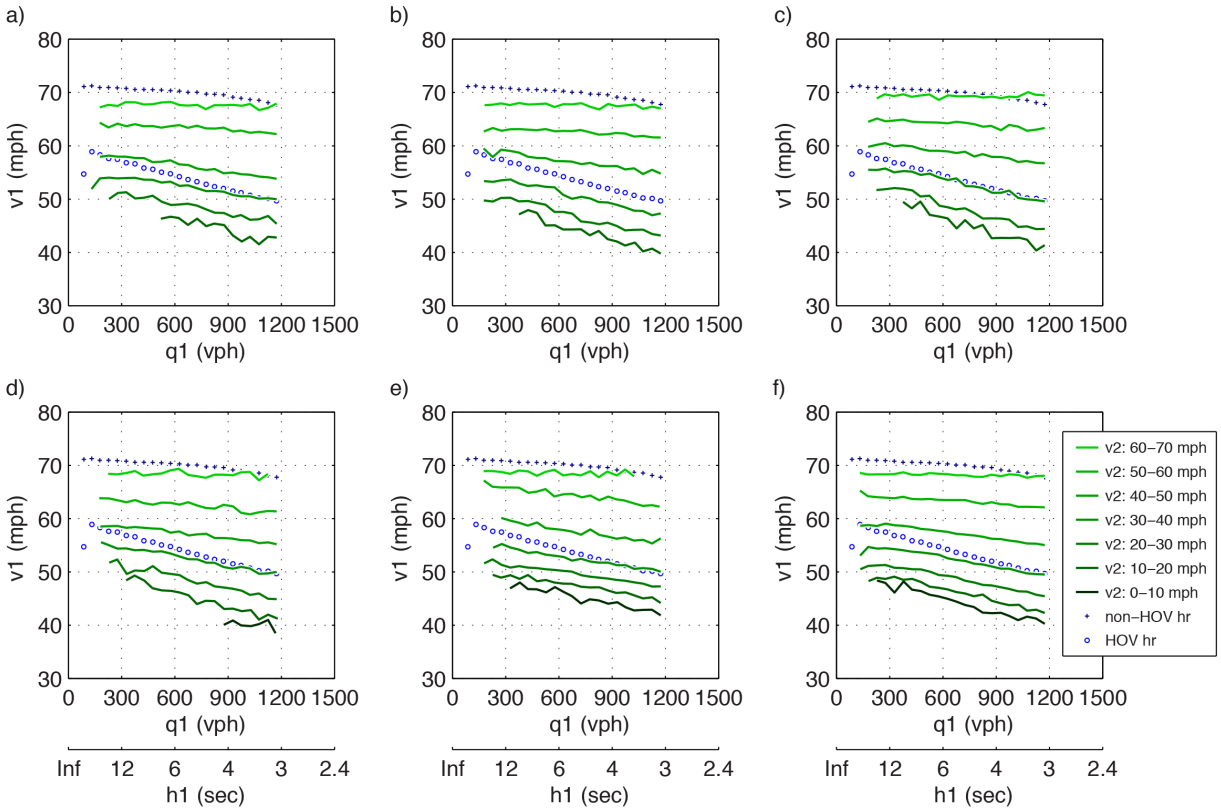

Figure 4, I-80 lane 1 eastbound vqFR for 18-22 ft vehicles during the HOV period sorted by v2 bins for (a) station 1, (b) station 2, (c) station 3, (d) station 4, (e) station 6, and (f) all stations combined.

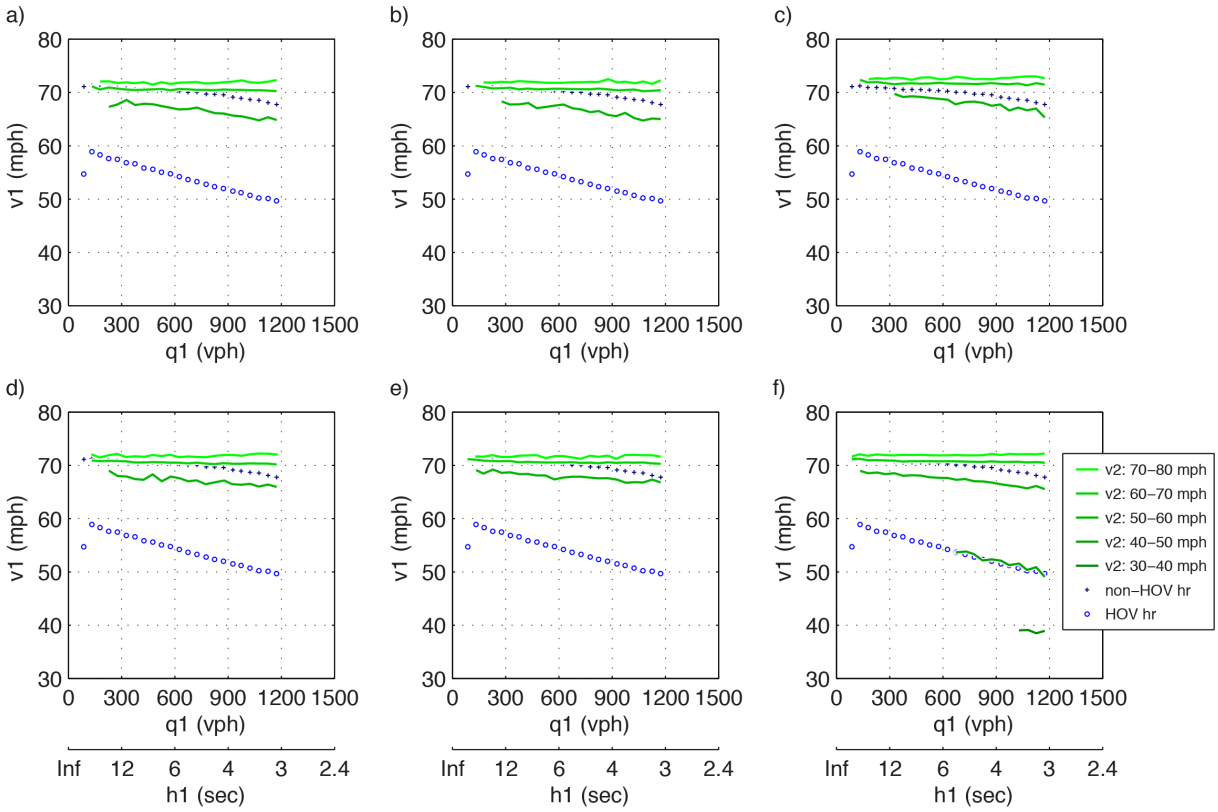

Figure 5, I-80 lane 1 eastbound vqFR for 18-22 ft vehicles during the non-HOV period sorted by v2 bins for (a) station 1, (b) station 2, (c) station 3, (d) station 4, (e) station 6, and (f) all stations combined.

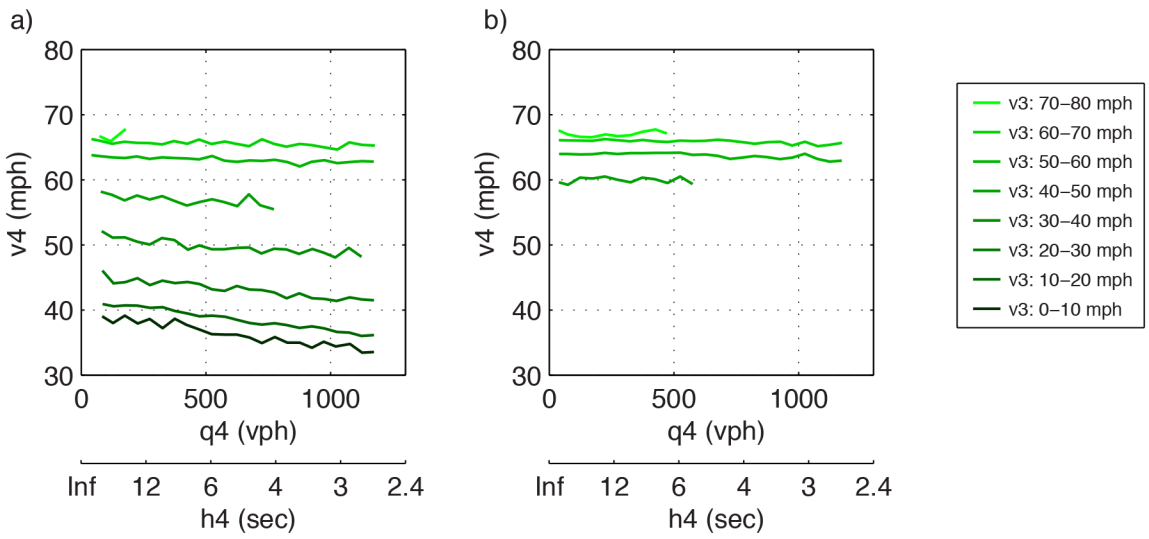

Figure 6, I-71 lane 4 northbound vqFR for 20.6-25.6 ft vehicles sorted by v3 bins for (a) the peak period, and (b) the non-peak period.

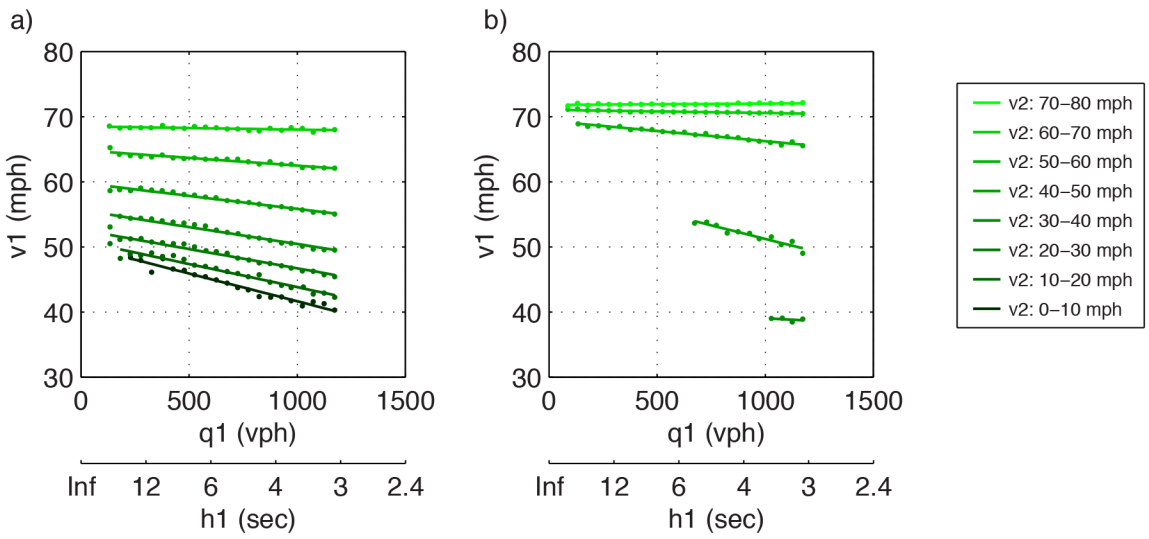

Figure 7, I-80 lane 1 eastbound vqFR linear regression models for 18-22 ft vehicles sorted by v2 bins across all stations combined during (a) the HOV period, and (b) the non-HOV period.

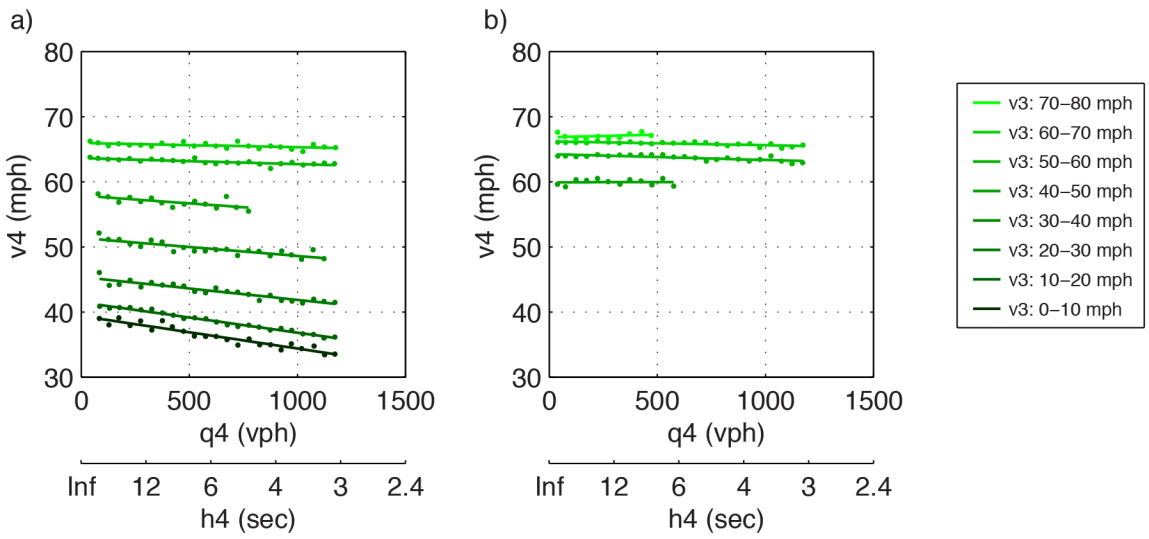

Figure 8, I-71 lane 4 northbound vqFR linear regression models for 20.6-25.6 ft vehicles sorted by v3 bins during (a) the peak period, and (b) the non-peak period.